

# A series of divalent metal complexes with mixed 5-(imidazol-1-ylmethyl)isophthalic acid and N-donor ligands: Synthesis, characterization and property



Hai-Wei Kuai<sup>a</sup>, Taka-aki Okamura<sup>b</sup>, Wei-Yin Sun<sup>a,\*</sup>

<sup>a</sup> Coordination Chemistry Institute, State Key Laboratory of Coordination Chemistry, School of Chemistry and Chemical Engineering, Nanjing National Laboratory of Microstructures, Nanjing University, Nanjing 210093, China

<sup>b</sup> Department of Macromolecular Science, Graduate School of Science, Osaka University, Toyonaka, Osaka 560-0043, Japan

## ARTICLE INFO

### Article history:

Received 30 November 2013

Accepted 18 January 2014

Available online 29 January 2014

### Keywords:

Copper(II)

Manganese(II)

Nickel(II)

Zinc(II)

Luminescence

Magnetic property

## ABSTRACT

Eight complexes with different 3d metal centers and auxiliary ligands, [Cu(L)(py)] (**1**), [Cu(L)(bpy)]·1.5H<sub>2</sub>O (**2**), [Mn(L)] (**3**), [Mn(L)(pybim)]·3H<sub>2</sub>O (**4**), [Ni(L)(bpy)]·2H<sub>2</sub>O (**5**), [Ni(L)(phen)]·2H<sub>2</sub>O (**6**), [Ni(L)(bpe)(H<sub>2</sub>O)]·2H<sub>2</sub>O (**7**) and [Zn(L)(bpy)]·2H<sub>2</sub>O (**8**) [H<sub>2</sub>L = 5-(imidazol-1-ylmethyl)isophthalic acid, py = pyridine, bpy = 2,2'-bipyridine, pybim = 2-(pyridin-2-yl)-1H-benzo[d]imidazole, phen = 1,10-phenanthroline, bpe = 1,2-di(pyridin-4-yl)ethylene] were obtained under hydrothermal conditions and characterized by single crystal and powder X-ray diffractions, IR, elemental and thermogravimetric analyses. Complex **1** is a 3-connected uninodal 2D network with (4.8<sup>2</sup>) topology, while **2**, **4**, **6** and **7** display 3-connected uninodal 2D network with (6<sup>3</sup>) **hcb** topology, **3** exhibits a (5,5)-connected binodal 3D net with (4<sup>5</sup>)(6<sup>5</sup>) topology, **5** and **8** have 1D double-chain structures. The influence of metal centers and auxiliary ligands on the structures of resultant complexes is discussed. Magnetic property of **3** and luminescence of **8** were investigated.

© 2014 Elsevier Ltd. All rights reserved.

## 1. Introduction

The assembling strategies of coordination architectures involve the deliberate design of organic building blocks and the adept employment of metal centers [1]. Hitherto, a lot of researches have been carried out to manage influential factors, including the coordination geometry of metal center, the intrinsic nature of organic ligand, and other experimental conditions such as acidic or basic media for the reaction system, reaction solvent, and temperature as well as the ratio of metal-to-ligand, to construct coordination supramolecular compounds for their fascinating structures and potential applications in gas storage, chemical sensors, ion exchange, microelectronics, magnetism, nonlinear optics, and heterogeneous catalysis etc. [2–5]. Among the above mentioned influential factors, the nature of organic ligand has been documented as crucial roles in the formation of coordination supramolecular compounds [6]. Therefore, the design of organic ligands is undoubtedly decisive in assembly of complexes. Among the well employed organic ligands, N- and/or O-donor multidentate ligands, such as isonicotinic acid, 4-(pyridin-4-yl)benzoic acid, and imidazole-4, 5-dicarboxylic acid, are always regarded as excellent building blocks for

construction of desirable frameworks and have been well employed in coordination chemistry due to their fine coordinating capacities and variable coordination modes [7].

In our previous studies, we ever used a series of imidazole-containing ligands, for example 1,3,5-tris(imidazol-1-yl)benzene and 1,3,5-tris(imidazol-1-ylmethyl)benzene, and mixed N- and O-donor containing ligands like 4-(imidazol-1-yl)benzoic acid and 3,5-di(imidazol-1-yl)benzoic acid to construct coordination supramolecular compounds [8]. Based on the previous studies, we have been recently focusing our attention on the utilization of the semi-rigid ligand 5-(imidazol-1-ylmethyl)isophthalic acid (H<sub>2</sub>L) as organic building blocks to react with varied metal salts under appropriate synthetic conditions. The H<sub>2</sub>L ligand possesses two carboxylate groups and one flexible imidazol-1-ylmethyl arm which can rotate freely. Hence, it could potentially adopt different conformation in assembly reaction *via* the adjustment of external experimental conditions. The H<sub>2</sub>L ligand can form series cadmium(II) and zinc(II) complexes with alkaline reagent dependent structural diversity; moreover, five cobalt(II) polymers from the H<sub>2</sub>L ligand were assembled and their structural diversity was achieved by the presence of auxiliary ligands and the alteration of metal-to-ligand ratio [9]. Based on the consideration of fact that functional properties of complexes are largely dependent on their architectures, more experimental conditions, including trying

\* Corresponding author. Tel.: +86 25 83593485; fax: +86 25 83314502.

E-mail address: [sunwy@nju.edu.cn](mailto:sunwy@nju.edu.cn) (W.-Y. Sun).

more types of auxiliary ligands and metal salts, were tried to further pursue structural diversity of complexes for the exploration of new crystalline materials.

In this paper, we report the preparation and structural characterization of a series of divalent 3d metal complexes: [Cu(L)(py)] (**1**), [Cu(L)(bpy)]·1.5H<sub>2</sub>O (**2**), [Mn(L)] (**3**), [Mn(L)(pybim)]·3H<sub>2</sub>O (**4**), [Ni(L)(bpy)]·2H<sub>2</sub>O (**5**), [Ni(L)(phen)]·2H<sub>2</sub>O (**6**), [Ni(L)(bpe)(H<sub>2</sub>O)]·2H<sub>2</sub>O (**7**) and [Zn(L)(bpy)]·2H<sub>2</sub>O (**8**) [H<sub>2</sub>L = 5-(imidazol-1-ylmethyl)isophthalic acid, py = pyridine, bpy = 2,2'-bipyridine, pybim = 2-(pyridin-2-yl)-1H-benzo[d]imidazole, phen = 1,10-phenanthroline, bpe = 1,2-di(pyridin-4-yl)ethylene]. The influential factors of synthetic strategies on structures will be discussed. In addition, magnetic property of **3** and luminescence of **8** were examined.

## 2. Experimental

### 2.1. Materials and measurements

All commercially available chemicals and solvents are of reagent grade and were used as received without further purification. The ligand H<sub>2</sub>L was prepared according to the previously reported method [9]. Elemental analyses of C, H, and N were taken

on a Perkin-Elmer 240C elemental analyzer. Infrared spectra (IR) were recorded on a Bruker Vector22 FT-IR spectrophotometer by using KBr pellets. Thermogravimetric analyses (TGA) were performed on a simultaneous SDT 2960 thermal analyzer under nitrogen atmosphere with a heating rate of 10 °C min<sup>-1</sup>. Powder X-ray diffraction (PXRD) patterns were measured on a Shimadzu XRD-6000 X-ray diffractometer with Cu Kα (λ = 1.5418 Å) radiation at room temperature. The magnetic measurement in the temperature range of 1.8–300 K was carried out on a Quantum Design MPMS7 SQUID magnetometer in a field of 2000 Oe. Diamagnetic corrections were made with Pascal's constants. The luminescence spectra for the powdered solid samples were measured on an Aminco Bowman Series 2 spectrofluorometer with a xenon arc lamp as the light source. In the measurements of emission and excitation spectra the pass width is 5 nm, and all the measurements were carried out under the same experimental conditions.

### 2.2. Preparation of [Cu(L)(py)] (**1**)

Reaction mixture of Cu(NO<sub>3</sub>)<sub>2</sub>·3H<sub>2</sub>O (24.1 mg, 0.1 mmol), H<sub>2</sub>L (24.6 mg, 0.1 mmol) and 1 mL pyridine in 10 mL H<sub>2</sub>O was sealed

**Table 1**  
Crystal data and structure refinements for complexes **1–8**.

Compound	<b>1</b>	<b>2</b>	<b>3</b>	<b>4</b>
Empirical formula	C <sub>17</sub> H <sub>13</sub> N <sub>3</sub> O <sub>4</sub> Cu	C <sub>44</sub> H <sub>38</sub> N <sub>8</sub> O <sub>11</sub> Cu <sub>2</sub>	C <sub>12</sub> H <sub>8</sub> N <sub>2</sub> O <sub>4</sub> Mn	C <sub>24</sub> H <sub>23</sub> N <sub>5</sub> O <sub>7</sub> Mn
Formula weight	386.84	981.90	299.14	548.41
Crystal system	orthorhombic	triclinic	monoclinic	triclinic
Space group	<i>Pbca</i>	<i>P</i> $\bar{1}$	<i>P</i> <sub>2</sub> / <i>c</i>	<i>P</i> $\bar{1}$
<i>a</i> (Å)	17.406(4)	9.5885(6)	8.8274(12)	8.753(8)
<i>b</i> (Å)	8.758(2)	9.8352(6)	16.682(2)	10.165(10)
<i>c</i> (Å)	20.774(7)	13.9055(9)	7.8691(11)	14.819(14)
α (°)	90.00	71.4010(10)	90.00	96.430(15)
β (°)	90.00	80.9910(10)	100.689(3)	91.546(15)
γ (°)	90.00	66.1990(10)	90.00	110.753(14)
<i>T</i> (K)	200	293(2)	293(2)	293(2)
<i>V</i> (Å <sup>3</sup> )	3166.9(16)	1136.58(12)	1138.7(3)	1222(2)
<i>Z</i>	8	1	4	2
<i>D</i> <sub>calc</sub> (g cm <sup>-3</sup> )	1.623	1.435	1.745	1.490
μ (mm <sup>-1</sup> )	1.408	1.003	1.171	0.595
<i>F</i> (000)	1576	504	604	566
θ Range (°)	3.05–27.49	1.55–26.00	2.35–27.00	1.39–28.00
Reflections collected	25700	6242	6508	8609
Unique reflections	3623	4373	2472	5845
Goodness-of-fit (GOF) on <i>F</i> <sup>2</sup>	1.092	1.074	1.367	1.053
<i>R</i> <sub>1</sub> <sup>a</sup> , <i>wR</i> <sub>2</sub> <sup>b</sup> [ <i>I</i> > 2σ( <i>I</i> )]	0.0416, 0.1076	0.0565, 0.1631	0.0995, 0.1815	0.0505, 0.1207
<i>R</i> <sub>1</sub> , <i>wR</i> <sub>2</sub> (all data)	0.0538, 0.1134	0.0631, 0.1692	0.1022, 0.1825	0.0694, 0.1304
Compound	<b>5</b>	<b>6</b>	<b>7</b>	<b>8</b>
Empirical formula	C <sub>22</sub> H <sub>20</sub> N <sub>4</sub> O <sub>6</sub> Ni	C <sub>24</sub> H <sub>20</sub> N <sub>4</sub> O <sub>6</sub> Ni	C <sub>24</sub> H <sub>24</sub> N <sub>4</sub> O <sub>7</sub> Ni	C <sub>22</sub> H <sub>20</sub> N <sub>4</sub> O <sub>6</sub> Zn
Formula weight	495.13	519.15	539.18	501.79
Crystal system	triclinic	triclinic	monoclinic	triclinic
Space group	<i>P</i> $\bar{1}$	<i>P</i> $\bar{1}$	<i>P</i> <sub>2</sub> / <i>c</i>	<i>P</i> $\bar{1}$
<i>a</i> (Å)	9.5783(7)	10.448(4)	9.9659(19)	9.4978(6)
<i>b</i> (Å)	10.1593(7)	14.664(4)	28.894(6)	10.2376(7)
<i>c</i> (Å)	13.0962(14)	15.179(4)	10.6565(14)	13.3159(13)
α (°)	97.7380(10)	79.215(10)	90.00	100.4420(10)
β (°)	100.3690(10)	78.396(13)	122.320(12)	98.5720(10)
γ (°)	116.8360(10)	85.013(11)	90.00	115.7140(10)
<i>T</i> (K)	293(2)	200	293(2)	293(2)
<i>V</i> (Å <sup>3</sup> )	1084.19(16)	2234.9(11)	2593.2(9)	1108.70(15)
<i>Z</i>	2	4	4	2
<i>D</i> <sub>calc</sub> (g cm <sup>-3</sup> )	1.517	1.543	1.381	1.503
μ (mm <sup>-1</sup> )	0.942	0.919	0.797	1.154
<i>F</i> (000)	512	1072	1120	516
θ Range (°)	1.63–25.99	3.06–27.48	2.37–28.00	1.61–26.00
Reflections collected	6015	21 127	16 051	6137
Unique reflections	4178	10 109	6138	4274
Goodness-of-fit (GOF) on <i>F</i> <sup>2</sup>	0.960	1.058	1.065	0.972
<i>R</i> <sub>1</sub> <sup>a</sup> , <i>wR</i> <sub>2</sub> <sup>b</sup> [ <i>I</i> > 2σ( <i>I</i> )]	0.0319, 0.0682	0.0437, 0.1144	0.0489, 0.1605	0.0507, 0.1263
<i>R</i> <sub>1</sub> , <i>wR</i> <sub>2</sub> (all data)	0.0394, 0.0708	0.0582, 0.1212	0.0625, 0.1668	0.0656, 0.1339

<sup>a</sup> *R*<sub>1</sub> = Σ||*F*<sub>o</sub>|| - ||*F*<sub>c</sub>||/Σ||*F*<sub>o</sub>||.

<sup>b</sup> *wR*<sub>2</sub> = [Σw(|*F*<sub>o</sub>|<sup>2</sup> - ||*F*<sub>c</sub>||<sup>2</sup>)/Σw(*F*<sub>o</sub>)<sup>2</sup>]<sup>1/2</sup>, where *w* = 1/[σ<sup>2</sup>(*F*<sub>o</sub>)<sup>2</sup> + (*aP*)<sup>2</sup> + *bP*]. *P* = (*F*<sub>o</sub><sup>2</sup> + 2*F*<sub>c</sub><sup>2</sup>)/3.

**Table 2**  
Selected bond lengths (Å) and bond angles (°) for complexes **1–8**<sup>a</sup>.

<b>1</b>			
Cu(1)–O(1)	1.9253(17)	Cu(1)–O(3)#1	1.9446(16)
Cu(1)–N(12)#2	1.991(2)	Cu(1)–N(21)	2.027(2)
O(1)–Cu(1)–O(3)#1	174.69(7)	O(1)–Cu(1)–N(12)#2	90.90(7)
O(3)#1–Cu(1)–N(12)#2	88.21(7)	O(1)–Cu(1)–N(21)	90.74(7)
O(3)#1–Cu(1)–N(21)	90.63(7)	N(12)#2–Cu(1)–N(21)	174.59(8)
<b>2</b>			
Cu(1)–N(3)	2.004(4)	Cu(1)–N(4)	2.157(4)
Cu(1)–N(11)	1.962(4)	Cu(1)–O(1)#1	1.977(3)
Cu(1)–O(3)#2	2.094(3)	N(3)–Cu(1)–N(11)	175.54(15)
N(3)–Cu(1)–N(4)	78.52(16)	O(3)#2–Cu(1)–N(3)	89.17(14)
O(1)#1–Cu(1)–N(3)	89.42(15)	N(4)–Cu(1)–N(11)	97.23(16)
O(3)#2–Cu(1)–N(11)	89.69(14)	O(3)#2–Cu(1)–N(4)	92.81(14)
O(1)#1–Cu(1)–N(4)	131.41(14)	O(1)#1–Cu(1)–N(11)	94.46(14)
O(1)#1–Cu(1)–O(3)#2	134.33(13)		
<b>3</b>			
Mn(1)–O(3)	2.098(5)	Mn(1)–O(1)#1	2.130(5)
Mn(1)–O(2)#2	2.067(5)	Mn(1)–N(12)#3	2.208(6)
Mn(1)–O(4)#4	2.090(5)	O(1)#1–Mn(1)–O(3)	91.76(19)
O(2)#2–Mn(1)–O(3)	96.2(2)	O(3)–Mn(1)–O(4)#4	142.3(2)
O(3)–Mn(1)–N(12)#3	85.0(2)	O(1)#1–Mn(1)–N(12)#3	162.6(2)
O(1)#1–Mn(1)–O(2)#2	93.5(2)	O(2)#2–Mn(1)–N(12)#3	103.8(2)
O(1)#1–Mn(1)–O(4)#4	85.8(2)	O(4)#4–Mn(1)–N(12)#3	86.4(2)
<b>4</b>			
Mn(1)–O(1)	2.220(2)	Mn(1)–N(11)#2	2.193(3)
Mn(1)–N(3)	2.364(3)	Mn(1)–N(4)	2.180(3)
Mn(1)–O(3)#1	2.186(3)	O(1)–Mn(1)–N(3)	136.06(9)
O(1)–Mn(1)–N(11)#2	94.52(9)	O(1)–Mn(1)–O(3)#1	86.85(10)
O(1)–Mn(1)–N(4)	94.72(9)	N(3)–Mn(1)–N(4)	73.21(10)
O(3)#1–Mn(1)–N(11)#2	95.61(9)	N(4)–Mn(1)–N(11)#2	162.43(8)
O(3)#1–Mn(1)–N(3)	136.24(8)	O(3)#1–Mn(1)–N(4)	99.80(9)
N(3)–Mn(1)–N(11)#2	89.81(11)		
<b>5</b>			
Ni(1)–N(3)	2.0545(17)	Ni(1)–N(4)	2.0535(17)
Ni(1)–N(11)	2.0508(17)	Ni(1)–O(1)#1	2.1709(14)
Ni(1)–O(2)#1	2.1300(13)	Ni(1)–O(3)#2	2.0201(13)
N(3)–Ni(1)–N(4)	79.58(7)	N(3)–Ni(1)–N(11)	178.13(7)
O(1)#1–Ni(1)–N(3)	92.86(6)	O(2)#1–Ni(1)–N(3)	91.36(6)
O(3)#2–Ni(1)–N(3)	91.54(6)	N(4)–Ni(1)–N(11)	98.84(7)
O(1)#1–Ni(1)–N(4)	155.40(6)	O(2)#1–Ni(1)–N(4)	95.30(6)
O(3)#2–Ni(1)–N(4)	104.61(6)	O(1)#1–Ni(1)–N(11)	88.99(6)
O(2)#1–Ni(1)–N(11)	89.78(6)	O(3)#2–Ni(1)–N(11)	87.88(6)
O(1)#1–Ni(1)–O(2)#1	61.24(5)	O(1)#1–Ni(1)–O(3)#2	98.92(6)
O(2)#1–Ni(1)–O(3)#2	160.08(5)		
<b>6</b>			
Ni(1)–O(1)	1.9907(16)	Ni(1)–O(5)	2.1891(16)
Ni(1)–O(6)	2.1333(15)	Ni(1)–N(1)	2.071(2)
Ni(1)–N(2)	2.070(2)	Ni(1)–N(12)#3	2.045(2)
Ni(2)–N(3)	2.064(2)	Ni(2)–N(4)	2.067(2)
Ni(2)–N(111)	2.039(2)	Ni(2)–O(7)#1	2.0209(16)
Ni(2)–O(3)#2	2.2254(16)	Ni(2)–O(4)#2	2.1226(16)
O(1)–Ni(1)–O(5)	97.84(7)	O(1)–Ni(1)–O(6)	158.84(7)
O(1)–Ni(1)–N(1)	105.93(7)	O(1)–Ni(1)–N(2)	90.59(8)
O(1)–Ni(1)–N(12)#3	91.78(8)	O(5)–Ni(1)–O(6)	61.01(6)
O(5)–Ni(1)–N(1)	155.06(7)	O(5)–Ni(1)–N(2)	92.40(7)
O(5)–Ni(1)–N(12)#3	89.53(7)	O(6)–Ni(1)–N(1)	95.12(7)
O(6)–Ni(1)–N(2)	90.94(7)	O(6)–Ni(1)–N(12)#3	87.67(7)
N(1)–Ni(1)–N(2)	80.08(8)	N(1)–Ni(1)–N(12)#3	97.08(8)
N(2)–Ni(1)–N(12)#3	176.72(8)	N(3)–Ni(2)–N(4)	80.16(9)
N(3)–Ni(2)–N(111)	97.13(8)	O(7)#1–Ni(2)–N(3)	107.58(7)
O(3)#2–Ni(2)–N(3)	153.30(7)	O(4)#2–Ni(2)–N(3)	93.52(7)
N(4)–Ni(2)–N(111)	176.90(8)	O(7)#1–Ni(2)–N(4)	88.48(8)
O(3)#2–Ni(2)–N(4)	93.55(8)	O(4)#2–Ni(2)–N(4)	92.91(7)
O(7)#1–Ni(2)–N(111)	90.92(8)	O(3)#2–Ni(2)–N(111)	89.55(7)
O(4)#2–Ni(2)–N(111)	88.75(7)	O(3)#2–Ni(2)–O(7)#1	98.09(6)
O(4)#2–Ni(2)–O(7)#1	158.76(6)	O(3)#2–Ni(2)–O(4)#2	60.67(6)

**Table 2** (continued)

<b>1</b>			
<b>7</b>			
Ni(1)–O(5)	2.046(2)	Ni(1)–N(3)	2.095(2)
Ni(1)–N(11)	2.078(2)	Ni(1)–O(1)#1	2.168(2)
Ni(1)–O(2)#1	2.097(2)	Ni(1)–O(3)#2	2.040(2)
O(5)–Ni(1)–N(3)	86.83(10)	O(5)–Ni(1)–N(11)	89.52(9)
O(1)#1–Ni(1)–O(5)	165.28(9)	O(2)#1–Ni(1)–O(5)	104.39(9)
O(3)#2–Ni(1)–O(5)	97.46(9)	N(3)–Ni(1)–N(11)	174.82(10)
O(1)#1–Ni(1)–N(3)	87.75(9)	O(2)#1–Ni(1)–N(3)	88.13(9)
O(3)#2–Ni(1)–N(3)	88.66(9)	O(1)#1–Ni(1)–N(11)	94.92(9)
O(2)#1–Ni(1)–N(11)	89.22(9)	O(3)#2–Ni(1)–N(11)	95.46(9)
O(1)#1–Ni(1)–O(2)#1	61.74(8)	O(1)#1–Ni(1)–O(3)#2	96.08(8)
O(2)#1–Ni(1)–O(3)#2	157.70(9)		
<b>8</b>			
Zn(1)–N(3)	2.141(3)	Zn(1)–N(4)	2.130(3)
Zn(1)–N(11)	2.104(3)	Zn(1)–O(1)#1	2.089(3)
Zn(1)–O(2)#1	2.466(3)	Zn(1)–O(3)#2	2.023(3)
N(3)–Zn(1)–N(4)	76.31(12)	N(3)–Zn(1)–N(11)	173.10(11)
O(1)#1–Zn(1)–N(3)	91.43(12)	O(2)#1–Zn(1)–N(3)	89.72(11)
O(3)#2–Zn(1)–N(3)	94.33(11)	N(4)–Zn(1)–N(11)	97.15(12)
O(1)#1–Zn(1)–N(4)	140.66(11)	O(2)#1–Zn(1)–N(4)	85.57(10)
O(3)#2–Zn(1)–N(4)	118.62(11)	O(1)#1–Zn(1)–N(11)	92.39(11)
O(2)#1–Zn(1)–N(11)	87.58(11)	O(3)#2–Zn(1)–N(11)	90.73(11)
O(1)#1–Zn(1)–O(2)#1	56.71(9)	O(1)#1–Zn(1)–O(3)#2	99.24(11)
O(2)#1–Zn(1)–O(3)#2	155.76(10)		

<sup>a</sup> Symmetry operators: #1  $x, 3/2 - y, 1/2 + z$ ; #2  $1 - x, 1 - y, 1 - z$  for **1**; for **2**, #1  $-1 + x, y, z$ ; #2  $-1 + x, 1 + y, z$ ; for **3**, #1  $-x, 1/2 + y, -1/2 - z$ ; #2  $-x, 2 - y, -1 - z$ ; #3  $1 - x, 2 - y, -z$ ; #4  $x, 5/2 - y, -1/2 + z$ ; for **4**, #1  $x, -1 + y, z$ ; #2  $1 + x, y, z$ ; for **5**, #1  $1 - x, -y, 1 - z$ ; #2  $1 - x, 1 - y, 1 - z$ ; for **6**, #1  $-1 + x, y, z$ ; #2  $x, y, 1 + z$ ; #3  $1 + x, y, z$ ; for **7**, #1  $-1 + x, y, -1 + z$ ; #2  $x, y, -1 + z$ ; for **8**, #1  $1 - x, -y, -z$ ; #2  $1 - x, 1 - y, -z$ .

in a 16 mL Teflon-lined stainless steel container and heated at 180 °C for 3 days. After cooling at a rate of 10 °C/h to the room temperature, purple block crystals of **1** were obtained in 45% yield. *Anal. Calc.* for  $C_{17}H_{13}N_3O_4Cu$ : C, 52.78; H, 3.39; N, 10.86. Found: C, 52.66; H, 3.66; N, 11.15%. IR (KBr pellet,  $cm^{-1}$ , Fig. S1): 3415 (w, br), 3111 (w), 1631 (s), 1612 (m), 1586 (m), 1520 (w), 1442 (w), 1352 (s), 1330 (s), 1096 (m), 833 (w), 769 (m), 744 (m), 725 (m), 707 (m), 655 (w).

### 2.3. Preparation of $[Cu(L)(bpy)] \cdot 1.5H_2O$ (**2**)

Reaction mixture of  $Cu(NO_3)_2 \cdot 3H_2O$  (24.1 mg, 0.1 mmol),  $H_2L$  (24.6 mg, 0.1 mmol), bpy (15.6 mg, 0.1 mmol), and KOH (11.2 mg, 0.2 mmol) in  $H_2O$  (10 mL) was sealed in a 16 mL Teflon-lined stainless steel container and heated at 180 °C for 3 days. After cooling at a rate of 10 °C/h to the room temperature, green block crystals of **2** were collected by filtration and washed by water and ethanol for several times with a yield of 32%. *Anal. Calc.* for  $C_{44}H_{38}N_8O_{11}Cu_2$ : C, 53.82; H, 3.90; N, 11.41. Found: C, 53.76; H, 3.62; N, 11.29%. IR (KBr pellet,  $cm^{-1}$ , Fig. S1): 3431 (m), 1614 (s), 1579 (s), 1443 (m), 1397 (m), 1357 (s), 1238 (w), 1095 (w), 765 (m), 720 (m).

### 2.4. Preparation of $[Mn(L)]$ (**3**)

Reaction mixture of  $MnCl_2 \cdot 4H_2O$  (19.8 mg, 0.1 mmol),  $H_2L$  (24.6 mg, 0.1 mmol), and KOH (11.2 mg, 0.2 mmol) in  $H_2O$  (10 mL) was sealed in a 16 mL Teflon-lined stainless steel container and heated at 180 °C for 3 days. After cooling at a rate of 10 °C/h to the room temperature, colorless block crystals of **3** were collected by filtration and washed by water and ethanol for several times with a yield of 39%. *Anal. Calc.* for  $C_{12}H_8N_2O_4Mn$ : C, 48.18; H, 2.70; N, 9.36. Found: C, 47.89; H, 2.42; N, 9.59%. IR (KBr pellet,  $cm^{-1}$ , Fig. S1): 3401 (w), 1626 (s), 1574 (s), 1541 (s), 1507 (s), 1449 (s), 1381 (s), 1336 (m), 1215 (m), 1108 (m), 1085 (m), 937 (m), 828 (m), 784 (s), 732 (s), 709 (s), 658 (m), 624 (m), 442 (m).

### 2.5. Preparation of [Mn(L)(pybim)]·3H<sub>2</sub>O (**4**)

Complex **4** was obtained by the same hydrothermal procedure as that used for synthesis of **3** except that pybim (18.2 mg, 0.1 mmol) was introduced into the reaction as auxiliary ligand. Colorless block crystals of **4** were collected by filtration and after washed by water and ethanol several times in 35% yield. *Anal. Calc.* for C<sub>24</sub>H<sub>23</sub>N<sub>5</sub>O<sub>7</sub>Mn: C, 52.56; H, 4.23; N, 12.77. Found: C, 52.81; H, 4.52; N, 12.59%. IR (KBr pellet, cm<sup>-1</sup>, Fig. S1): 3420 (w), 1620 (s), 1568 (s), 1441 (m), 1376 (s), 1325 (w), 1287 (w), 1235 (w), 1108 (w), 979 (w), 940 (w), 781 (w), 748 (s).

### 2.6. Preparation of [Ni(L)(bpy)]·2H<sub>2</sub>O (**5**)

Complex **5** was obtained by the same procedure as that used for preparation of **2** except that Ni(NO<sub>3</sub>)<sub>2</sub>·6H<sub>2</sub>O (29.1 mg, 0.1 mmol) was used. After cooling at a rate of 10 °C/h to the room temperature, green block crystals of **5** were collected by filtration and washed by water and ethanol for several times with a yield of 42%. *Anal. Calc.* for C<sub>22</sub>H<sub>20</sub>N<sub>4</sub>O<sub>6</sub>Ni: C, 53.37; H, 4.07; N, 11.32. Found: C, 53.56; H, 4.32; N, 11.50%. IR (KBr pellet, cm<sup>-1</sup>, Fig. S1): 3432 (m), 1613 (s), 1588 (s), 1550 (s), 1441 (s), 1370 (s), 1287 (w), 1088 (m), 1024 (w), 940 (w), 838 (w), 768 (m), 723 (m), 659 (m).

### 2.7. Preparation of [Ni(L)(phen)]·2H<sub>2</sub>O (**6**)

The title complex was obtained by the same hydrothermal procedure as that used for synthesis of **5** except that phen (18.0 mg, 0.1 mmol) was used instead of bpy. After cooling at a rate of 10 °C/h to the room temperature, aqua-blue platelet crystals of **6** were collected by filtration and washed by water and ethanol for several times with a yield of 37%. *Anal. Calc.* for C<sub>24</sub>H<sub>20</sub>N<sub>4</sub>O<sub>6</sub>Ni: C, 55.53; H, 3.88; N, 10.79. Found: C, 55.31; H, 4.06; N, 10.50%. IR (KBr pellet, cm<sup>-1</sup>, Fig. S1): 3452 (m), 1620 (s), 1582 (m), 1550 (s), 1517 (m), 1428 (m), 1364 (s), 1287 (w), 1101 (m), 940 (w), 851 (m), 781 (m), 723 (s), 666 (w).

### 2.8. Preparation of [Ni(L)(bpe)(H<sub>2</sub>O)]·2H<sub>2</sub>O (**7**)

Complex **7** was prepared by the same hydrothermal procedure as that used for synthesis of **5** except that bpe (18.2 mg, 0.1 mmol) was used instead of bpy. Green block crystals of **7** were collected by filtration and after washed by water and ethanol several times in 52% yield. *Anal. Calc.* for C<sub>24</sub>H<sub>24</sub>N<sub>4</sub>O<sub>7</sub>Ni: C, 53.46; H, 4.49; N, 10.39. Found: C, 53.71; H, 4.22; N, 10.16%. IR (KBr pellet, cm<sup>-1</sup>, Fig. S1): 3471 (m), 1613 (s), 1543 (s), 1459 (m), 1376 (s), 1280 (w), 1094 (m), 1024 (w), 832 (m), 781 (m), 748 (m), 723 (m), 666 (w), 634 (w), 550 (m).

### 2.9. Preparation of [Zn(L)(bpy)]·2H<sub>2</sub>O (**8**)

Complex **8** was obtained by the same hydrothermal procedure as that used for synthesis of **5** except that Zn(NO<sub>3</sub>)<sub>2</sub>·6H<sub>2</sub>O (29.7 mg, 0.1 mmol) was used. Colorless block crystals of **8** were isolated by filtration and washed by water and ethanol several times in 52% yield. *Anal. Calc.* for C<sub>22</sub>H<sub>20</sub>N<sub>4</sub>O<sub>6</sub>Zn: C, 52.65; H, 4.02; N, 11.16. Found: C, 52.59; H, 3.93; N, 11.29%. IR (KBr pellet, cm<sup>-1</sup>, Fig. S1): 3442 (m), 1623 (s), 1580 (s), 1545 (s), 1439 (s), 1366 (s), 1283 (w), 1083 (m), 1022 (w), 938 (w), 842 (w), 766 (m), 728 (m), 651 (m).

### 2.10. X-ray crystallography

The X-ray diffraction data for **1** and **6** were collected on a Rigaku Rapid II imaging plate area detector with Mo K $\alpha$  radiation

( $\lambda = 0.71075 \text{ \AA}$ ) using MicroMax-007HF microfocus rotating anode X-ray generator and VariMax-Mo optics at 200 K. Their structures were solved by direct methods with SIR92 [10] and expanded using Fourier techniques [11]. The crystallographic data collections for **2–5**, and **7–8** were carried out on a Bruker Smart Apex CCD area-detector diffractometer using graphite-monochromated Mo K $\alpha$  radiation ( $\lambda = 0.71073 \text{ \AA}$ ) at 293 K. The diffraction data were integrated by using the SAINT program [12], which was also used for the intensity corrections for the Lorentz and polarization effects. Semi-empirical absorption correction was applied using the SADABS program [13]. The structures were solved by direct methods and all non-hydrogen atoms were refined anisotropically on  $F^2$  by the full-matrix least-squares technique using the SHELXL-97 crystallographic software package [14]. In **1–8**, all hydrogen atoms attached to the C atoms are generated geometrically, and the ones of O6 in **2**, O7 and O8 in **7** could not be located and thus were excluded from the refinement, while the rest hydrogen atoms of water or N atom of pybim in **4** were found at reasonable position in the difference Fourier maps and located there. The details of crystal parameters, data collection, and refinements for the complexes are summarized in Table 1, selected bond lengths and angles are listed in Table 2.

## 3. Results and discussion

### 3.1. Crystal structure description of [Cu(L)(py)] (**1**)

The result of single crystal X-ray diffraction analysis revealed that **1** crystallizes in orthorhombic *Pbca* space group. The asymmetric unit of **1** consists of one Cu(II), one L<sup>2-</sup> and one coordinated pyridine molecule. Each Cu(II) atom is four-coordinated with distorted square planar coordination geometry by two carboxylate oxygen and one imidazolyl nitrogen atoms from three different L<sup>2-</sup> ligands, and one pyridine nitrogen atom (Fig. 1a). The bond distances vary from 1.9253 (17) to 2.027 (2) Å and the bond angles around the Cu(II) atom are in the range of 88.21(7)–174.69(7)° (Table 2). Two carboxylate groups in the L<sup>2-</sup> ligand link two metal ions each with  $\mu_1-\eta^1:\eta^0$ -monodentate coordination mode (Scheme 1A). The alternate linkage of the L<sup>2-</sup> to Cu(II) forms an infinite one-dimensional (1D) chain by ignoring the coordination of imidazolyl group (Fig. 1b). If taking the coordination of imidazolyl group into consideration, the 1D chains are further jointed together to form an interesting sandwich-like two-dimensional (2D) network (Fig. 1c and 1d). The sandwich-like 2D architecture consists of upper and lower two layers defined by benzene ring planes of L<sup>2-</sup> ligand with imidazolyl groups filled between the two layers. While the pyridine molecules are stuck onto the external surface of 2D network. Within the double-layer 2D network of **1**, the distance of the upper and the lower layers is 5.15 Å, the nearest distance of two parallel pyridine molecules is 8.76 Å and interestingly, the nearest distance of two parallel imidazolyl groups also equals 8.76 Å. For the better insight on the nature of 2D network, suitable nodes and connectors can be defined by using a topological approach. As mentioned above, each L<sup>2-</sup> ligand bridges three different Cu(II) and each Cu(II) is also coordinated by three different L<sup>2-</sup> ligands. Thus, both of Cu(II) and L<sup>2-</sup> can be regarded as 3-connected nodes, thus **1** displays a 3-connected uninodal 2D network with Point (Schläfli) symbol of (4.8<sup>2</sup>) (Fig. 1e) [15].

### 3.2. Crystal structure description of [Cu(L)(bpy)]·1.5H<sub>2</sub>O (**2**), [Mn(L)(pybim)]·3H<sub>2</sub>O (**4**), and [Ni(L)(phen)]·2H<sub>2</sub>O (**6**)

Complexes **2**, **4** and **6** crystallize in the same triclinic crystal system *P-1* space group and show similar structural feature, thus only the structure of **2** is described here in detail while the ones of **4** and **6** are given in Figs. S2 and S3.

As shown in Fig. 2a, each Cu(II) is five-coordinated with distorted trigonal bipyramidal coordination geometry by two carboxylate oxygen atoms from two different  $L^{2-}$  ligands with average Cu–O bond distance of 2.036 Å, three nitrogen atoms from one bpy molecule and one imidazolyl group of  $L^{2-}$  with average Cu–N

bond distance of 2.041 Å. The coordination bond angles around Cu(II) vary from 78.52(16) to 175.54(15)° (Table 2). The equatorial plane is defined by one bpy nitrogen and two carboxylate oxygen atoms, while the other two nitrogen ones occupy the axial positions. Both carboxylate groups of  $L^{2-}$  in **2** adopt  $\mu_1\text{-}\eta^1\text{:}\eta^0\text{-}$

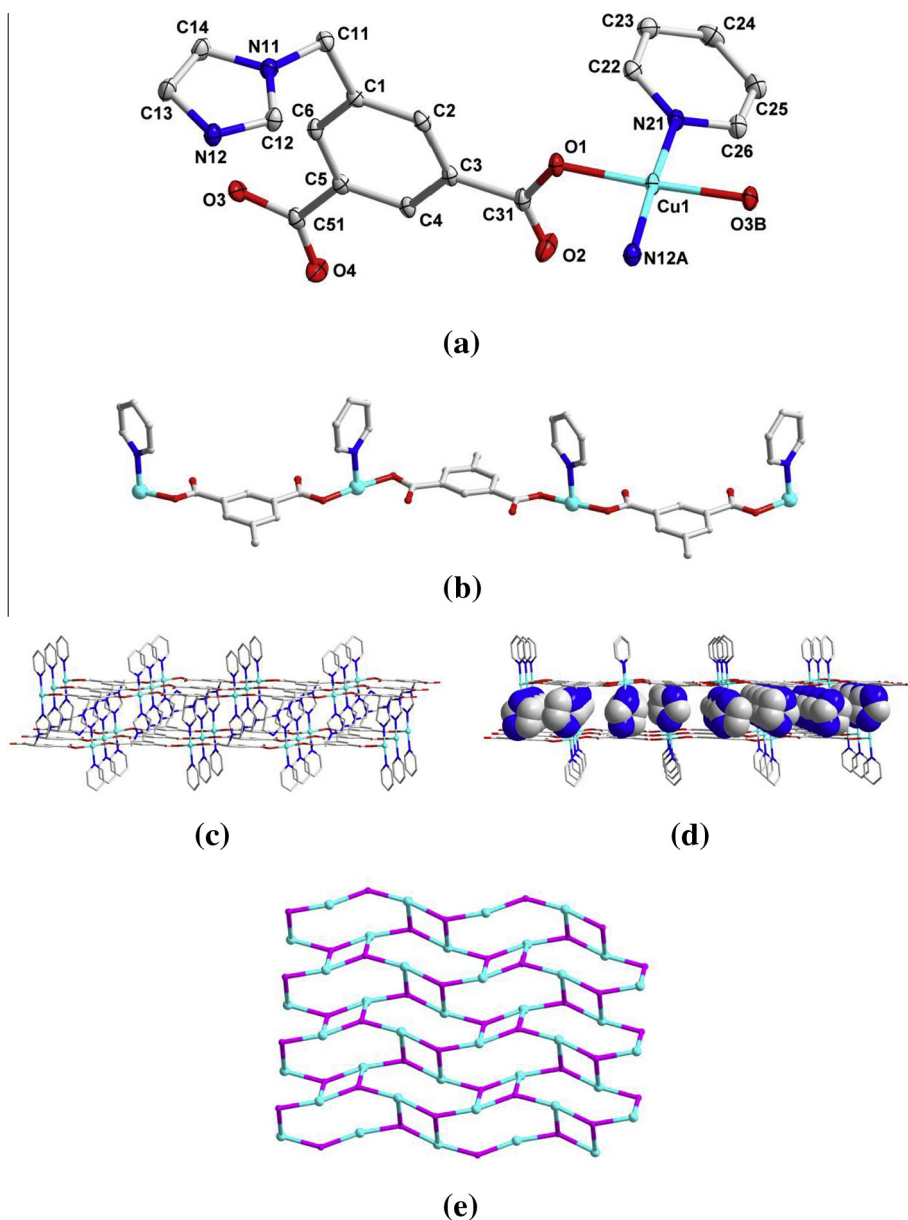
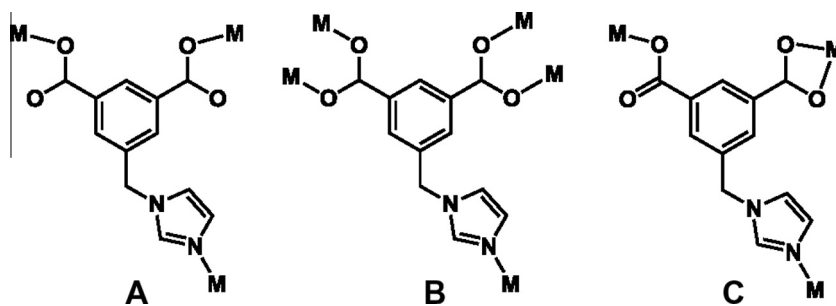


**Fig. 1.** (a) The coordination environment of Cu(II) in **1** with the ellipsoids drawn at the 30% probability level. The hydrogen atoms are omitted for clarity. (b) 1D chain structure in **1**. (c) 2D network of **1**. (d) 2D network of **1** with imidazole groups shown in space-filling mode. (e) Schematic representation of the uninodal 3-connected 2D ( $4.8^2$ ) network of **1**.



**Scheme 1.** Coordination modes of the  $L^{2-}$  appeared in **1–8**.

monodentate mode (Scheme 1A) and each  $L^{2-}$  ligand connects three different Cu(II) atoms and in turn each Cu(II) is coordinated by three different  $L^{2-}$  ligands. Such kind of interconnections repeats infinitely to form a 2D network (Fig. 2b). Both  $L^{2-}$  and Cu(II) in **2** can be regarded as 3-connectors, thus the network of **2** can be simplified into a uninodal 3-connected 2D ( $6^3$ ) **hcb** network (Fig. 2c).

### 3.3. Crystal structure description of $[Mn(L)]$ (**3**)

As shown in Fig. 3a, each Mn(II) is five-coordinated by four carboxylate oxygen atoms from four different  $L^{2-}$  ligands with average Mn–O bond distance of 2.096 Å, and one imidazolyl nitrogen atom with Mn–N bond distance of 2.208(6) Å to furnish distorted trigonal bipyramidal coordination geometry. Both of two carboxylate groups

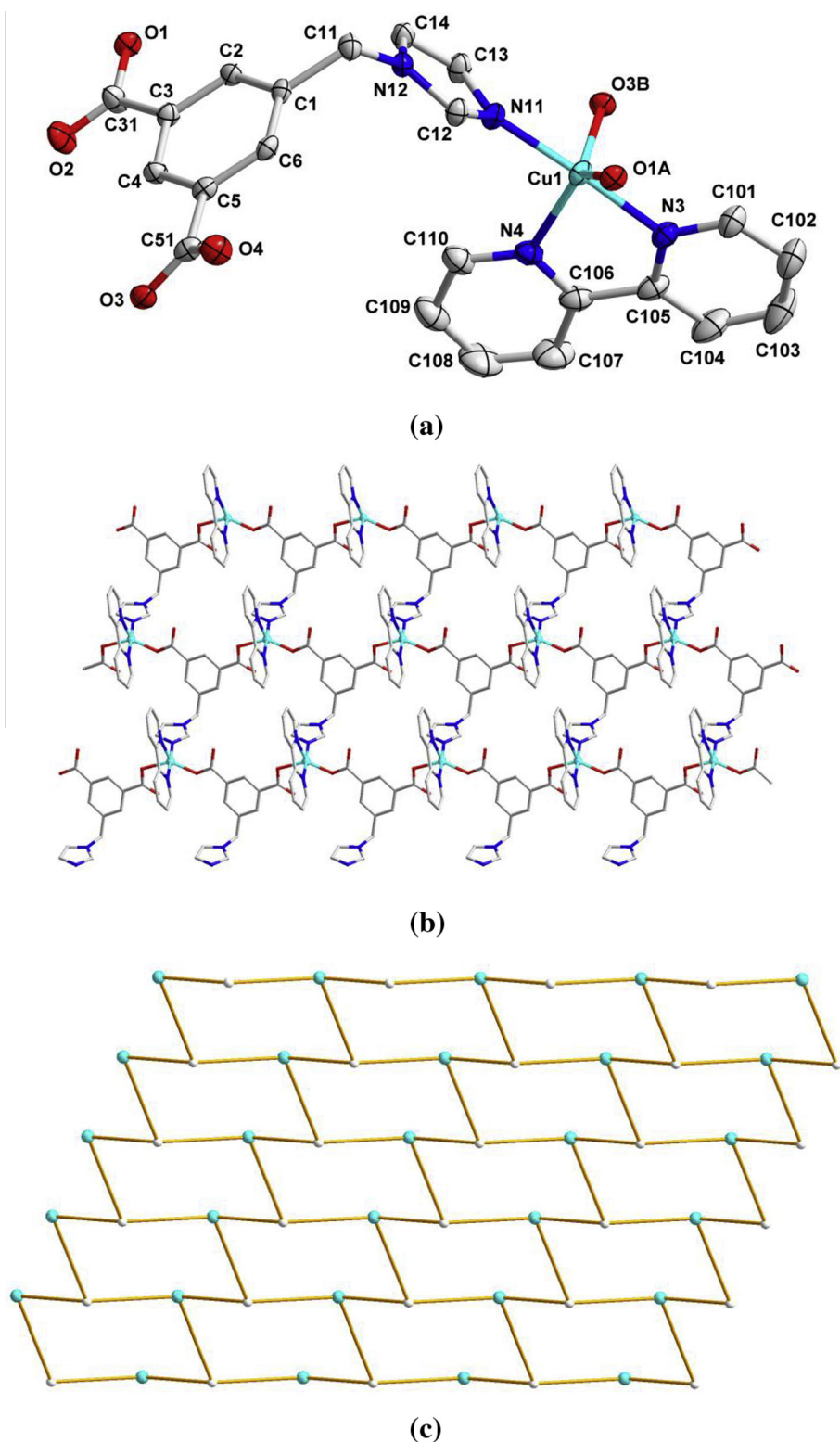


**Fig. 2.** (a) The coordination environment of Cu(II) in **2** with the ellipsoids drawn at the 30% probability level. The hydrogen atoms and free water molecules are omitted for clarity. (b) 2D network of **2**. (c) Schematic representation of uninodal 3-connected **hcb** network of **2** with  $6^3$  topology.

of  $L^{2-}$  ligand in **3** adopt  $\mu_2\text{-}\eta^1\text{:}\eta^1$ -bridging coordination mode (Scheme 1B). Thus, each  $L^{2-}$  ligand links five different Mn(II) atoms and each Mn(II) is coordinated by five different  $L^{2-}$  ligands. Such kind of linkage expands infinitely to produce a three-dimensional (3D) framework of **3** (Fig. 3b), in which 2D layer structure can be isolated if the coordination of imidazolyl group is ignored (Fig. 3c). From topological view, both  $L^{2-}$  ligand and metal center can be regarded as 5-connected nodes, and thus **3** can be described as a (5,5)-connected binodal 3D framework with  $(4^5)(6^5)$  topology (Fig. 3d).

#### 3.4. Crystal structure description of $[\text{Ni}(\text{L})(\text{bpy})]\cdot 2\text{H}_2\text{O}$ (**5**) and $[\text{Zn}(\text{L})(\text{bpy})]\cdot 2\text{H}_2\text{O}$ (**8**)

The same space group and similar cell parameters as listed in Table 1 imply that **5** and **8** are isomorphous and isostructural, thus only **5** is used for detailed structural description. The coordination environment around Ni(II) atom is shown in Fig. 4a with atom numbering scheme. Ni1 is six-coordinated with a distorted

octahedral coordination geometry by three nitrogen atoms (N3, N4, and N11) from coordinated bpy molecule and imidazolyl group of  $L^{2-}$  with average Ni-N bond distance of 2.053 Å and three carboxylate oxygen ones from two different  $L^{2-}$  ligand with average Ni-O bond length of 2.107 Å. Two carboxylate groups in each  $L^{2-}$  ligand adopt  $\mu_1\text{-}\eta^1\text{:}\eta^0$ -monodentate and  $\mu_1\text{-}\eta^1\text{:}\eta^1$ -chelating coordination modes, respectively. The  $L^{2-}$  ligand in **5** can be described as tridentate coordination mode using its two carboxylate and one imidazolyl groups (Scheme 1C). The infinite interconnections of  $L^{2-}$  ligands and metal centers form neutral double-stranded chain structure. Interestingly, within the double-chain flexible  $L^{2-}$  ligand spiral around a dummy column to exhibit a tube-like structure (Fig. 4b).

#### 3.5. Crystal structure description of $[\text{Ni}(\text{L})(\text{bpe})(\text{H}_2\text{O})]\cdot 2\text{H}_2\text{O}$ (**7**)

Each Ni(II) is six-coordinated by four oxygen and two nitrogen atoms to furnish a distorted octahedral coordination geometry

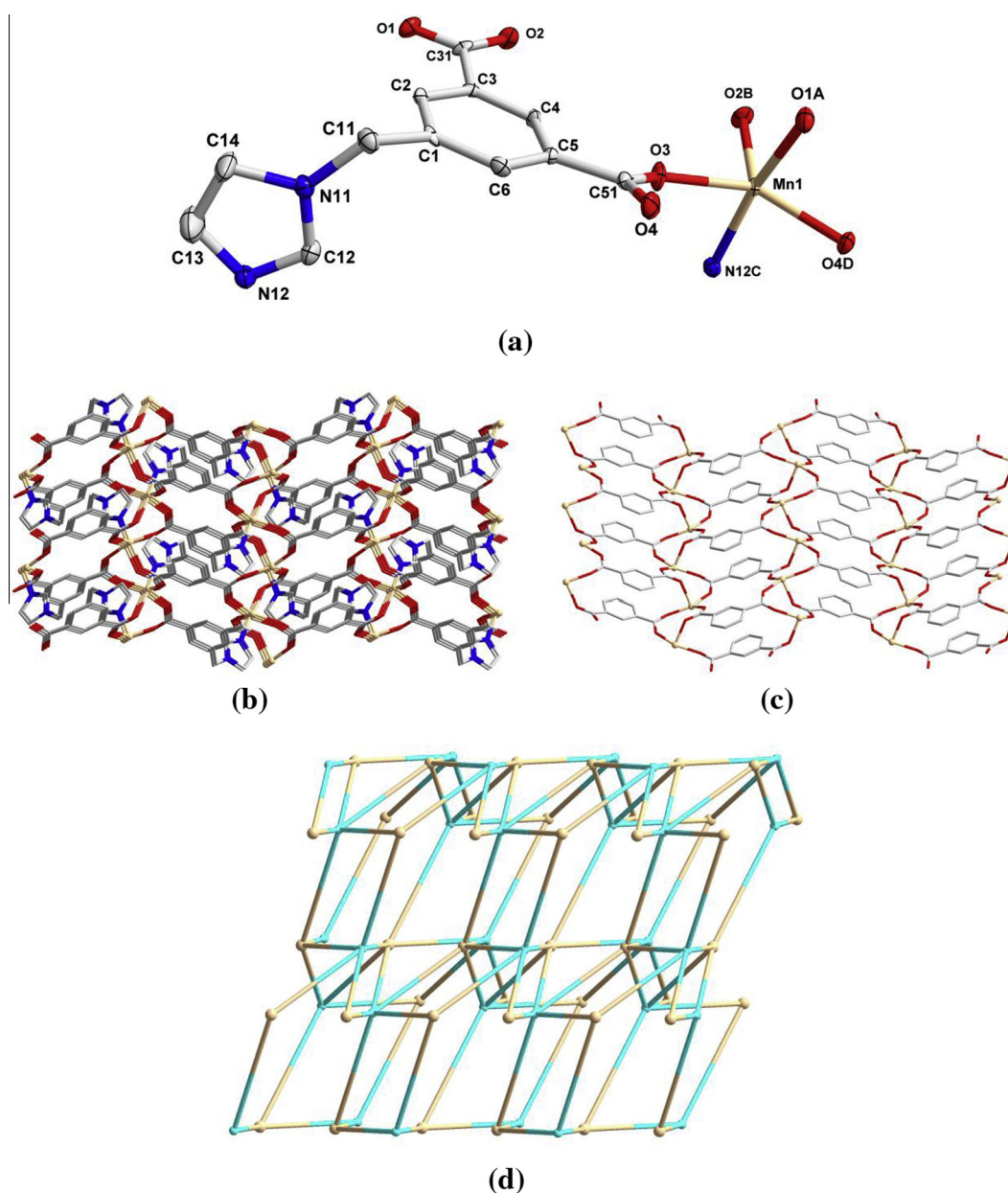


**Fig. 3.** (a) The coordination environment of Mn(II) in **3** with the ellipsoids drawn at the 30% probability level. The hydrogen atoms are omitted for clarity. (b) 3D structure of **3**. (c) The 2D network in **3**. (d) The schematic representations of the binodal (5,5)-connected 3D net of **3** with  $(4^5)(6^5)$  topology: smaller,  $L^{2-}$  ligand; larger, Mn(II).

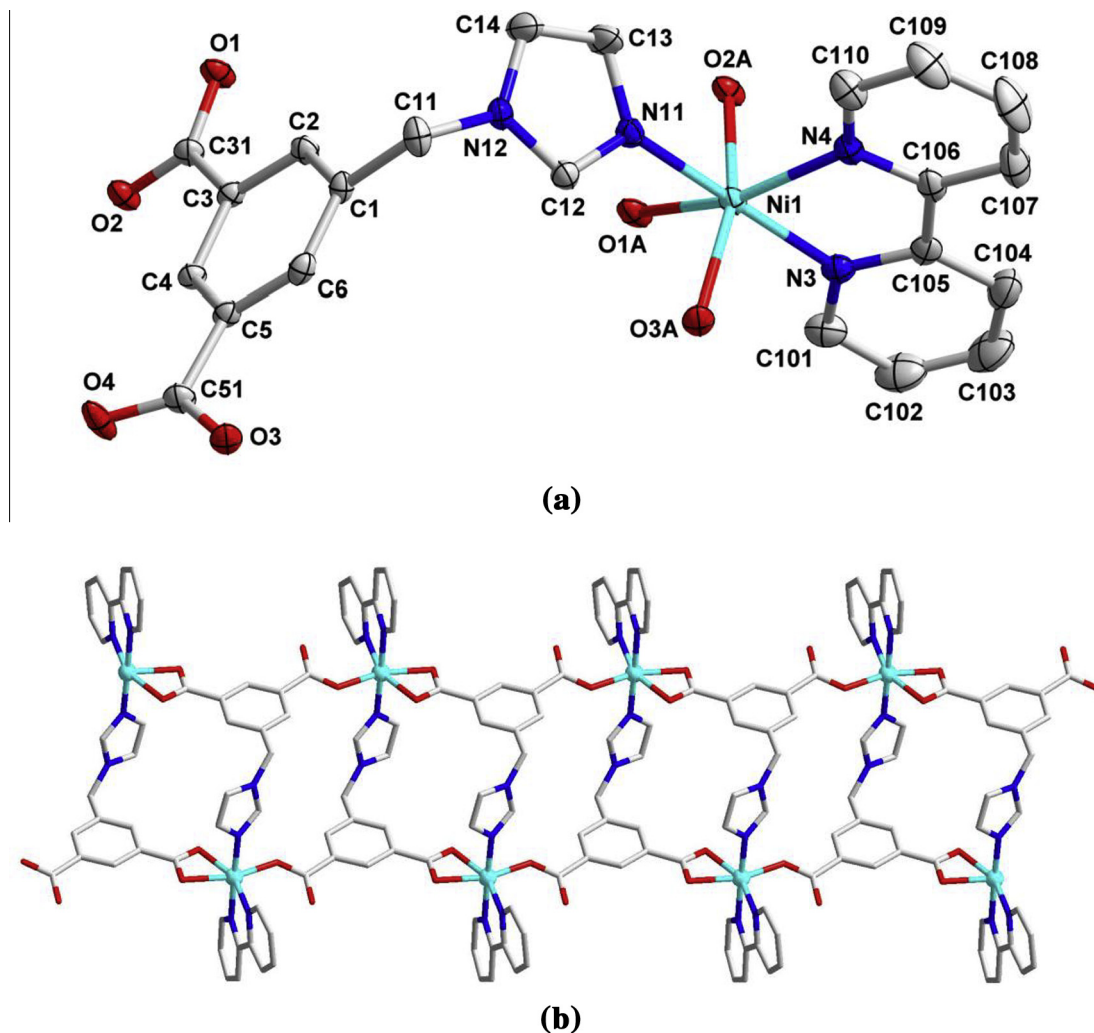


**Fig. 4.** (a) The coordination environment of Ni(II) in **5** with the ellipsoids drawn at the 30% probability level. The hydrogen atoms and free water molecules are omitted for clarity. (b) The 1D double chain of **5**.

(Fig. 5a). It is noteworthy that the co-ligand bpe just acts as a terminal ligand in **7** with one of the pyridine group free of coordination. Two carboxylate groups of  $L^{2-}$  adopt  $\mu_1\text{-}\eta^1\text{:}\eta^0$ -monodentate and  $\mu_1\text{-}\eta^1\text{:}\eta^1$ -chelating coordination modes (Scheme 1C). Each  $L^{2-}$  ligand connects three different Ni(II) atoms and each Ni(II) is also coordinated by three different  $L^{2-}$  ligands. Such coordination mode makes **7** a 2D network structure (Fig. 5b), which can be viewed as a stairway-like network with bpe molecules standing on it (Fig. 5c). As mentioned above, both of  $L^{2-}$  and Ni(II) in **7** can be regarded as 3-connected nodes, thus the network of **7** can be regarded as a uninodal 3-connected 2D hcb network with  $(6^3)$  topology (Fig. 5d). The 2D networks are further joined together by hydrogen bonding interactions to generate a 3D supramolecular framework (Fig. 5e). The hydrogen bonding data for **7** are summarized in Table S1.

### 3.6. Preparation and structural comparison of complexes **1–8**

Copper(II), manganese(II), nickel(II) and zinc(II) salts were employed as metal sources to react with  $H_2L$  ligand under hydrothermal conditions at 180 °C in the presence (or absence) of N-donor auxiliary ligands (Scheme 2), as a result, complexes **1–8** were obtained. The pure phase of the synthesized **1–8** was confirmed by powder X-ray diffraction (PXRD) measurements. As shown in

Fig. S4, each PXRD pattern of the as-synthesized sample is consistent with the simulated one.

The structures of **1–8** vary from 1D chain to 3D architecture. Two copper complexes display different structural feature, which is closely related with the introduction of pyridine and bpy molecules into their respective reaction system. Within manganese and nickel complexes series, auxiliary ligands are responsible for their structural diversity. Apart from co-ligands, metal centers may have subtle impact on the formation of complexes. For example, **2** and **5** show metal-controlled structural diversity, while **5** and **9** are just isomorphous and isostructural.

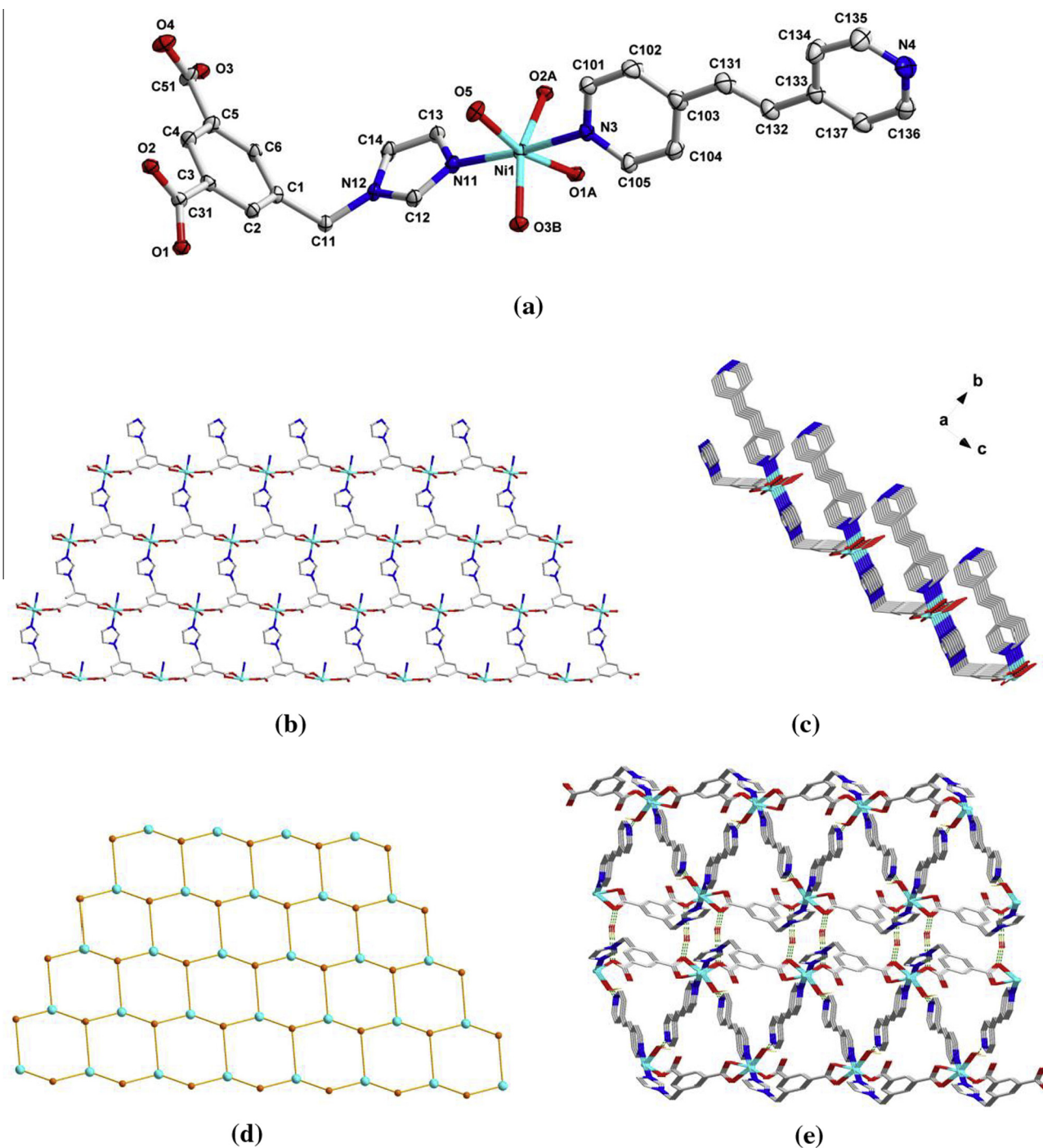
To further comprehend the coordination chemistry of M(II) complexes with the imidazole and carboxylate-containing ligand, structural comparison of **1–8** with our previously reported Co(II), Zn(II) and Cd(II) complexes was carried out [9]. All the complexes in the present and previously reported work were synthesized via hydrothermal methods. However, different reaction conditions result in structural diversity. Complex **1** was obtained from the mixed solvent of pyridine and water. Pyridine not only acts as alkaline reagent for deprotonation of  $H_2L$  but also takes part in coordination. The situation is similar to the Cd(II) complex which is also synthesized in the mixture of pyridine and water. However, these two complexes have 1D and 2D structures, respectively. Structural diversity may closely relate with metal centers. Complex **3** and the

Cd(II) complex were synthesized in the absence of any auxiliary ligand and under almost the same reaction conditions: the same 180 °C reaction temperature and the same KOH for deprotonation, but show different 2D and 3D structures, which may be caused by the different metal centers [9a]. A Co(II) complex was formed in the presence of pybim as auxiliary ligand [9b] showing (6<sup>3</sup>) 2D **hcb** network and is isostructural to Mn(II) complex **4**. Co-ligand phen was used to construct Co(II) and Ni(II) complexes (**6**) with the same six-coordination numbers, exhibiting 1D and 2D structures dependent on metal centers. Co-ligand bpe in **7** and the Co(II) one display different coordination modes: in **7** just as monodentate

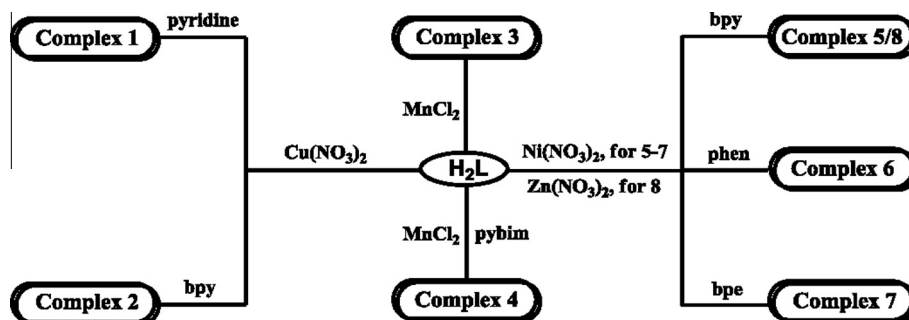
ligand, but in the Co(II) complex as bridging ligand. Their structures are respective 2D network and 2D + 2D → 3D parallel interpenetration of slabs. The results imply that the auxiliary ligand, metal centers have remarkable impact on the structure of the resultant complexes.

### 3.7. Thermal stability of complexes 1–8

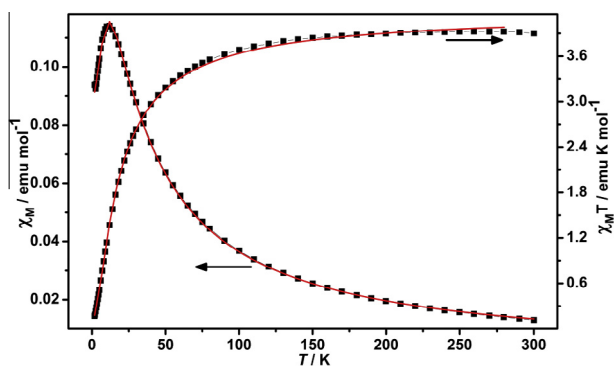
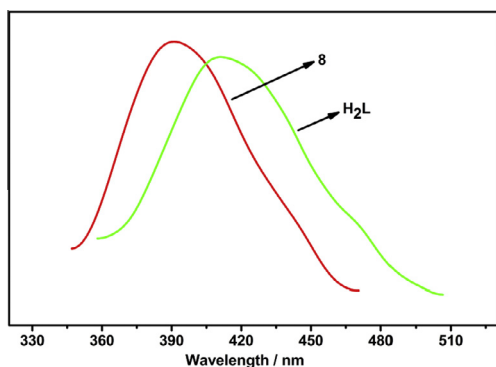
Complexes **1–8** were subjected to thermogravimetric analysis (TGA) to ascertain their thermal stability, and the TGA curves of **1–8** are shown in Fig. S5. It is clear that no obvious weight loss



**Fig. 5.** (a) The coordination environment of Ni(II) in **7** with the ellipsoids drawn at the 30% probability level. The hydrogen atoms and lattice water molecules are omitted for clarity. (b) 2D network of **7**. (c) Ladder-like 2D layer structure of **7**. (d) The schematic representations of the uninodal 3-connected 2D (6<sup>3</sup>) **hcb** net of **7**. (e) The 3D extended architecture of **7** with hydrogen bonding interactions indicated by dashed lines.



Scheme 2. Schematic representation for synthesis of 1–8.

Fig. 6. Temperature dependences of magnetic susceptibility of  $\chi_M$ , and  $\chi_{MT}$  for **3**. The solid lines represent the fitted curves.Fig. 7. Emission spectra of **8** and  $H_2L$  in the solid state at room temperature.

was observed before the decomposition of the frameworks occurred at about 282 °C for **1** and 522 °C for **3**, which further confirms no solvent in their structures. For other six complexes, the weight losses in the temperature range of 89–134 °C for **2**, 73–135 °C for **4**, 87–124 °C for **5**, 83–113 °C for **6**, 89–145 °C for **7**, and 111–155 °C for **8** correspond to the release of water molecules with the observed values of 5.36% for **2**, 9.96% for **4**, 7.42% for **5**, 6.70% for **6**, 10.16% for **7**, and 7.36% for **8** which are close to the calculated ones of 5.50%, 9.85%, 7.27%, 6.93%, 10.02%, and 7.17%, respectively. The decomposition of frameworks starts at 252 °C for **2**, 315 °C for **4**, 375 °C for **5**, 417 °C for **6**, 362 °C for **7**, and 380 °C for **8**.

### 3.8. Magnetic property of **3**

The Mn(II) atoms are bridged by carboxylate groups to form 1D Mn(II)-carboxylate chains in **3** with the nearest Mn···Mn distance

of 4.14 Å, which might mediate magnetic interactions [16]. Therefore, the magnetic property of **3** was investigated over the temperature range of 1.8–300 K with a 2000 Oe applied magnetic field. The magnetic behavior of **3** in the form of  $\chi_M$ ,  $\chi_M^{-1}$ , and  $\chi_{MT}$  versus  $T$  is depicted in Fig. 6. The  $\chi_{MT}$  value of 3.90 emu K mol<sup>-1</sup> at 300 K is lower than the value expected for magnetically isolated Mn(II) atom (4.38 emu K mol<sup>-1</sup>,  $g = 2.0$ ). As the temperature is lowered, the  $\chi_{MT}$  value decreases continuously; while the  $\chi_M$  value increases smoothly to reach maximum of 0.115 emu mol<sup>-1</sup> at 10.4 K and then decreases steeply. The  $\chi_M^{-1}$  value (above 50 K) obeys the Curie–Weiss law well with a Weiss constant ( $\theta$ ) of –12.12 K and a Curie constant ( $C$ ) of 4.11 emu K mol<sup>-1</sup> (Fig. S6). The negative value of  $\theta$  and the shape of the  $\chi_{MT}$  versus  $T$  curve suggest there may exist antiferromagnetic interactions between the neighboring Mn(II) centers [17]. In order to estimate the strength of the magnetic interactions in **3**, the following equation was used [18]:

$$\chi_{MT} = A \exp(-E_1/kT) + B \exp(-E_2/kT)$$

Here,  $A + B$  equals the curie constant ( $C$ ), and  $E_1, E_2$  represent the activation energies corresponding to the spin–orbit coupling and the magnetic exchange interaction, respectively. The obtained values of  $A + B = 4.19$  cm<sup>3</sup> mol<sup>-1</sup> K and  $E_1/k = 15.94$  K agree with those given in a previous report [18]. The value of  $-E_2/k = -1.80$  K, corresponding to  $J = -3.60$ , further proved that the antiferromagnetic interactions exist between neighboring Mn(II) [19].

### 3.9. Luminescent property of **8**

Previously studies have shown that inorganic–organic hybrid coordination polymers containing metal centers with  $d^{10}$  electron configuration, such as Zn(II), exhibited excellent luminescent properties and may have potential applications as photoactive materials [20]. In the present work, the photoluminescence of complex **8** and  $H_2L$  ligand has been preliminarily investigated in the solid state at room temperature. As shown in Fig. 7, intensive photoluminescence emission can be observed under the experimental condition for complex **8** and  $H_2L$  ligand with emission bands at 392 nm ( $\lambda_{ex} = 347$  nm) for **8** and 412 nm ( $\lambda_{ex} = 361$  nm) for  $H_2L$  ligand. The fluorescent emission of **8** may be tentatively assigned to ligand emission due to their similarity [21]. The observation of blue shift of the emission maximum in **8** compared with free  $H_2L$  ligand may originate from the coordination of the ligands to the metal centers [22].

## 4. Conclusion

Eight new complexes have been successfully synthesized through the hydrothermal reactions of Cu(II), Mn(II), Ni(II) and Zn(II) salts with bifunctional ligand  $H_2L$ . Structural diversity is achieved by means of the presence of different N-donor auxiliary

ligands. The results also imply that metal centers can subtly impact the formation of complexes. Investigation of magnetic behaviors of **3** shows that there exist antiferromagnetic interactions between the neighboring Mn(II) centers and zinc complex **8** exhibits strong luminescence.

## Acknowledgements

This work was financially supported by the National Natural Science Foundation of China (Grant Nos. 91122001 and 21331002) and the National Basic Research Program of China (Grant No. 2010CB923303).

## Appendix A. Supplementary data

CCDC 970769–970776 contain the supplementary crystallographic data for **1–8**. These data can be obtained free of charge via <http://www.ccdc.cam.ac.uk/conts/retrieving.html>, or from the Cambridge Crystallographic Data Centre, 12 Union Road, Cambridge CB2 1EZ, UK; fax: +44 1223 336 033; or e-mail: deposit@ccdc.cam.ac.uk. Supplementary data associated with this article can be found, in the online version, at <http://dx.doi.org/10.1016/j.poly.2014.01.019>.

## References

- (a) T.R. Cook, Y.R. Zheng, P.J. Stang, *Chem. Rev.* 113 (2013) 734;  
(b) J.P. Zhang, Y.B. Zhang, J.B. Lin, X.M. Chen, *Chem. Rev.* 112 (2012) 1001;  
(c) J.M. Jia, S.J. Liu, Y. Cui, S.D. Han, T.L. Hu, X.H. Bu, *Cryst. Growth Des.* 13 (2013) 4631;  
(d) N. Stock, S. Biswas, *Chem. Rev.* 112 (2012) 933;  
(e) Z.H. Chen, Y. Zhao, P. Wang, S.S. Chen, W.Y. Sun, *Polyhedron* 67 (2014) 253.
- (a) M. Juricek, P.H.J. Kouwer, A.E. Rowan, *Chem. Commun.* 47 (2011) 8740;  
(b) L. Luo, G.C. Lv, P. Wang, Q. Liu, K. Chen, W.Y. Sun, *CrystEngComm* 15 (2013) 9537;  
(c) L. Luo, K. Chen, Q. Liu, Y. Lu, T.A. Okamura, G.C. Lv, Y. Zhao, W.Y. Sun, *Cryst. Growth Des.* 13 (2013) 2312.
- (a) S. Hazra, S. Bhattacharya, M.K. Singh, L. Carrella, E. Rentschler, T. Weyhermueller, G. Rajaraman, S. Mohanta, *Inorg. Chem.* 52 (2013) 12881;  
(b) C.N. Verani, *J. Inorg. Biochem.* 106 (2012) 59;  
(c) Y. Zhao, X. Zhou, T.A. Okamura, M. Chen, Y. Lu, W.Y. Sun, J.Q. Yu, *Dalton Trans.* 41 (2012) 5889.
- (a) P. Chakraborty, A. Guha, S. Das, E. Zangrando, D. Das, *Polyhedron* 49 (2013) 12;  
(b) P. Wang, L. Luo, J. Fan, G.C. Lv, Y. Song, W.Y. Sun, *Microporous Mesoporous Mater.* 175 (2013) 116;  
(c) A.W. Salman, R.A. Haque, S. Budagumpi, H.Z. Zulikha, *Polyhedron* 49 (2013) 200.
- (a) C.F. Wang, G.L. Dai, Z.N. Jin, *Inorg. Chim. Acta* 394 (2013) 255;  
(b) H.B. Duan, X.M. Ren, Q.J. Meng, *Coord. Chem. Rev.* 254 (2010) 1509.
- (a) Z.H. Chen, Y. Zhao, S.S. Chen, P. Wang, W.Y. Sun, *J. Solid State Chem.* 202 (2013) 215;  
(b) K.L. Zhang, C.T. Hou, J.J. Song, Y. Deng, L. Li, S.W. Ng, G.W. Diao, *CrystEngComm* 14 (2012) 590;  
(c) K.L. Zhang, Y. Chang, J.B. Zhang, Y. Deng, T.T. Qiu, L. Li, S.W. Ng, *CrystEngComm* 14 (2012) 2926.
- (a) S.S. Chen, M. Chen, S. Takamizawa, M.S. Chen, Z. Su, W.Y. Sun, *Chem. Commun.* 47 (2011) 752;  
(b) S.S. Chen, M. Chen, S. Takamizawa, P. Wang, G.C. Lv, W.Y. Sun, *Chem. Commun.* 47 (2011) 4902;  
(c) M.S. Chen, M. Chen, S. Takamizawa, T. Okamura, J. Fan, W.Y. Sun, *Chem. Commun.* 47 (2011) 3787;  
(d) Z. Su, J. Fan, W.Y. Sun, *Inorg. Chem. Commun.* 27 (2013) 18.
- (a) Z. Su, J. Fan, M. Chen, T.A. Okamura, W.Y. Sun, *Cryst. Growth Des.* 11 (2011) 1159;  
(b) Z. Su, G.C. Lv, J. Fan, G.X. Liu, W.Y. Sun, *Inorg. Chem. Commun.* 15 (2012) 317;  
(c) Z. Su, Y. Song, Z.S. Bai, J. Fan, G.X. Liu, W.Y. Sun, *CrystEngComm* 12 (2010) 4339;  
(d) Z. Su, J. Fan, W.Y. Sun, *Inorg. Chem. Commun.* 27 (2013) 18;  
(e) J. Fan, H.F. Zhu, T.A. Okamura, W.Y. Sun, W.X. Tang, N. Ueyama, *Chem. Eur. J.* 9 (2003) 4724.
- (a) H.W. Kuai, J. Fan, Q. Liu, W.Y. Sun, *CrystEngComm* 14 (2012) 3708;  
(b) H.W. Kuai, C. Hou, W.Y. Sun, *Polyhedron* 52 (2013) 1268.
- SIR92: A. Altomare, G. Casciaro, C. Giacovazzo, A. Guagliardi, M. Burla, G. Polidori, M. Camalli, *J. Appl. Crystallogr.* 27 (1994) 435.
- P.T. Beurskens, G. Admiraal, G. Beurskens, W.P. Bosman, R. de Gelder, R. Israel, J.M.M. Smits, The DIRFID-99 Program System; Technical Report of the Crystallography Laboratory, University of Nijmegen, Nijmegen, The Netherlands, 1999.
- Bruker AXS Inc, SAINT, Program for Data Extraction and Reduction, Bruker AXS Inc, Madison, WI, 2001.
- G.M. Sheldrick, SADABS, Program for Bruker Area Detector Absorption Correction, University of Göttingen, Göttingen, Germany, 1997.
- (a) G.M. Sheldrick, SHELXS-97, Programs for Solution of Crystal Structure, University of Göttingen, Germany, 1997;  
(b) G.M. Sheldrick, SHELXL-97, Programs of Refinement for Crystal Structure, University of Göttingen, Germany, 1997.
- (a) V.A. Blatov, *IUCr CompComm Newlett.* 7 (2006) 4;  
(b) V.A. Blatov, TOPOS, A Multipurpose Crystallochemical Analysis with the Program Package, Samara State University, Russia, 2009.
- D. Ghoshal, G. Mostafa, T.K. Maji, E. Zangrando, T.H. Lu, J. Ribas, N.R. Chaudhuri, *New J. Chem.* 28 (2004) 1204.
- M. Wang, C.B. Ma, H.S. Wang, C.N. Chen, Q.T. Liu, *J. Mol. Struct.* 873 (2008) 94.
- (a) J.M. Rueff, N. Masciocchi, P. Rabu, A. Sironi, A. Skoulios, *Chem. Eur. J.* 8 (2002) 1813;  
(b) Z. Su, Z.S. Bai, J. Xu, T.A. Okamura, G.X. Liu, Q. Chu, X.F. Wang, W.Y. Sun, N. Ueyama, *CrystEngComm* 11 (2009) 873;  
(c) C.B. Ma, C.N. Chen, Q.T. Liu, D.Z. Liao, L.C. Li, L.C. Sun, *New J. Chem.* 27 (2003) 890.
- (a) R.L. Carlin, *Magnetochemistry*, Springer, Berlin, Heidelberg, 1986;  
(b) O. Kahn, *Molecular Magnetism*, VCH, Weinheim, 1993;  
(c) S.M. Humphrey, R.A. Mole, J.M. Rawson, P.T. Wood, *Dalton Trans.* (2004) 1670.
- (a) Y. Yang, P. Du, Y.Y. Liu, J.F. Ma, *Cryst. Growth Des.* 13 (2013) 4781;  
(b) D. Volz, D.M. Zink, T. Bockrocker, J. Friedrichs, M. Nieger, T. Baumann, U. Lemmer, *Chem. Mater.* 25 (2013) 3414.
- (a) B. Valeur, *Molecular Fluorescence. Principles and Applications*, Wiley-VCH, Weinheim, Germany, 2002;  
(b) Y.Q. Huang, B. Ding, H.B. Song, B. Zhao, P. Ren, P. Cheng, H.G. Wang, D.Z. Liao, S.P. Yan, *Chem. Commun.* (2006) 4906.
- (a) X.L. Wang, Y.F. Bi, G.C. Liu, H.Y. Lin, T.L. Hu, X.H. Bu, *CrystEngComm* 10 (2008) 349;  
(b) L. Zhang, Z.J. Li, Q.P. Lin, Y.Y. Qin, J. Zhang, P.X. Yin, J.K. Cheng, Y.G. Yao, *Inorg. Chem.* 48 (2009) 6517.